CHAPTER 8

Monitoring Saharan Aerosol Transport by Means of Atmospheric Turbidity Measurements

J. M. PROSPERO, D. L. SAVOIE, T. N. CARLSON, and R. T. NEES

ABSTRACT

Atmospheric turbidity measurements were made in two spectral bands (500 nm and 880 nm) in a network of five land stations and ten ships distributed across the northern Equatorial Atlantic during the GARP Atlantic Tropical Experiment (GATE) during the summer of 1974. The turbidities were high off the coast of Africa and decreased toward the west. The mean Volz turbidities (B_{500}) at Sal Island, Barbados, and Miami were: 0.297, 0.130, and 0.100. The values at 880 nm were: 0.250, 0.114, and 0.062. The central and eastern Atlantic turbidities are equal to those of large, heavily industrialized cities. The mean Angstrom wavelength exponent α at these three stations was: 0.348, 0.285, and 0.899. Low values of α indicate that neutral extinction obtains which is consistent with the appearance of the sky in this region. High values of α (i.e. values greater than one) were consistently observed only at Miami and only when Saharan aerosols were not present in the atmosphere. The consistently low α values at all stations in the presence of Saharan air parcels suggests that the optically effective portion of the aerosol size distribution does not change substantially during transit across the Atlantic. The daily mean station turbidities do not seem to be correlated in any simple way with the daily average mineral aerosol concentrations measured in surface level air at the stations.

8.1 INTRODUCTION

In 1974, a large scale aerosol program was carried out as a part of the Global Atmospheric Research Program (GARP) Atlantic Tropical Experiment (GATE). One of the principal objectives was to investigate the geographical distribution of aerosols with respect to meteorological parameters over the entire equatorial North Atlantic Ocean. To this end, we established an aerosol and atmospheric turbidity network which consisted of five land stations and ten ship stations. The design and operation of this network was closely coordinated with a solar radiation program

carried out by T. N. Carlson at Sal Island, one of the network stations situated off the coast of Africa. At this time, we present the turbidity data and some supporting aerosol data from this network.

8.2 SITE DESCRIPTIONS

The land stations in this network were: Dakar, Senegal (14°44′N, 17°33′W); Sal Island, Cape Verde Islands (16°45′N, 22°57′W); Barbados, West Indies (13°10′N, 59°25′W); Miami, Florida, U.S.A. (25°45′N, 80°15′W); Bermuda (32°19′N, 64°46′W).

The Dakar aerosol site was situated on the coast at Pointe des Almadies, 12 km northwest of the city proper. Photometer measurements were usually made at the airport at Yoff, 4 km east of the coastal site.

Sal Island is the northeasternmost island of the Cape Verde Archipelago and is situated 600 km west–northwest of Dakar. The aerosol sampler was positioned on the crest of a hill 26 m above sea level and 500 m from the eastern shoreline.

Barbados, the easternmost island of the West Indies arc, is 3900 km west of Sal. The sampling site is located on a 20 m coral rock bluff on the east coast. Photometer measurements were made at a site 4 km west of the sampling site.

The Miami station is situated on the eastern side of Virginia Key, a small island about 4 km east of the city of Miami. The sampler was placed on the roof of a building 20 m above ground level and 25 m above sea level. Photometer measurements were made within a few hundred yards of this station.

The Bermuda measurements were made at the aerosol station operated by R. Duce (U. of Rhode Island) on the western tip of the island.

The ten ships in the network were: R/V Gilliss (U.S.), R/V Endurer (U.K.), R/V Charterer (U.K.), R/V Jean Charcot (France), R/V Sirius (Brazil), R/V Saldanha (Brazil), R/V Matamoros (Mexico), R/V Dallas (U.S.), R/V Researcher (U.S.), and R/V Oceanographer (U.S.). Ships were assigned fixed stations for each of the three experimental phases of GATE.

8.3 MEASUREMENT OF ATMOSPHERIC TURBIDITY

Atmospheric turbidity is defined as the extinction of solar radiation by suspended particles that are large with respect to the wavelength of light; that is, particles with radii from about 0.1 to 10 μm. The measurement of turbidity is important because it integrates the total loading of aerosol in the atmosphere on the line between the sun and the detector. There are several turbidity indices in existence; in this work we use the Volz turbidity, B, which is defined as:

$$I_\lambda \cdot S = I_{0\lambda}\, 10 \exp -\frac{P}{P_0}(\tau_{R\lambda} + \tau_{0\lambda} + B_\lambda)M \qquad (1)$$

where:

I_λ = irradiance at wavelength λ at the observing point,
$I_{0\lambda}$ = extraterrestrial irradiance at λ at the mean sun-earth distance,
S = correction factor for the mean sun-earth distance,
$\tau_{R\lambda}$ = Raleigh scattering coefficient for air molecules at λ,
$\tau_{0\lambda}$ = absorption coefficient for ozone at λ,
B_λ = extinction coefficient for aerosols at λ,
M = optical air mass,
P = station pressure,
P_0 = standard pressure at sea level.

The values of S for each day of the year can be calculated or obtained from a table. $\tau_{R\lambda}$ and $\tau_{0\lambda}$ are also known and M can be calculated or measured directly by the instrument. Thus, with the known calibration constant for the instrument, $I_{0\lambda}$, the aerosol optical thickness (Volz turbidity) can be calculated:

$$B_\lambda = \frac{\log (I_{0\lambda}/I_\lambda \cdot S)}{M} - (\tau_{R\lambda} + \tau_{0\lambda}) \tag{2}$$

The turbidity is often expressed for base e: $\tau_d = 2.303\, B_\lambda$.

Another useful turbidity parameter is Angstrom's wavelength exponent, α, for total haze scattering where scattering, σ, is given by:

$$\sigma \sim \lambda^{-\alpha} \tag{3}$$

Alpha can be calculated from turbidity measurements at any two wavelengths:

$$\alpha = \ln (B_{\lambda_1}/B_{\lambda_2})/\ln (\lambda_2/\lambda_1) \tag{4}$$

The value of α is determined by the size distribution of the aerosol. Typical continental (non arid-region) aerosols have α's of one to two; arid region aerosols have α's close to zero.

The sun photometers which we used (except as noted below) were manufactured by F. E. Volz. These have two channels, green and red. The green channel has an absorption type filter with a λ_{eff} of 500 nm and a 60 nm half width. The red channel has an interference filter with a λ_{eff} of 880 nm and 35 nm half width. The field of view is 3°. A silicon photovoltaic detector is employed.

8.4 PHOTOMETER CALIBRATION

The evaluation of sunphotometer data from a specific instrument is dependent on the knowledge of the extraterrestrial irradiance value ($I_{0\lambda}$) for that instrument. In practice, $I_{0\lambda}$ is obtained by Langley plots on days with constant low turbidity. Readings are taken throughout the day and log I is plotted against air mass

TABLE 8.1 Mean Atmospheric Turbidity Parameters for the North Atlantic during GATE (All Stations: Summer, 1974)

Site (Photometer No.) Parameters	*B*(500)		*B*(880)		Alpha		Lat (°N)	Long (°W)	*n*
LAND:									
BARBADOS (No. 281)									
Average (SD)	0.130	(0.081)	0.114	(0.076)	0.285	(0.244)	13.17	59.42	84
Geometric Mean (GSD)	0.106	(1.955)	0.090	(2.087)					
BERMUDA (No. 32)									
Average (SD)	0.097	(0.053)	0.041	(0.025)	1.618	(0.473)	32.32	64.77	59
Geometric Mean (GSD)	0.090	(1.407)	0.036	(1.552)					
DAKAR (No. 278)									
Average (SD)	0.350	(0.125)	0.328	(0.133)	0.152	(0.210)	14.73	17.55	12
Geometric Mean (GSD)	0.330	(1.434)	0.303	(1.547)					
MIAMI (No. 101)									
Average (SD)	0.100	(0.050)	0.062	(0.038)	0.899	(0.403)	25.75	80.25	81
Geometric Mean (GSD)	0.090	(1.545)	0.054	(1.661)					
SAL (No. 273)									
Average (SD)	0.305	(0.117)	0.253	(0.113)	0.368	(0.180)	16.75	22.95	33
Geometric Mean (GSD)	0.281	(1.566)	0.227	(1.679)					
SAL (No. 276)									
Average (SD)	0.266	(0.103)	0.221	(0.093)	0.353	(0.148)	16.75	22.95	45
Geometric Mean (GSD)	0.244	(1.562)	0.200	(1.653)					
SAL (EPPLEY)									
Average (SD)	0.273	(0.109)					16.75	22.95	30
Geometric Mean (GSD)	0.252	(1.518)							

SHIP:									
DALLAS (EPPLEY No. 55)									
Average (SD)	0.062	(0.036)					8.53	24.41	33
Geometric Mean (GSD)	0.052	(1.874)							
CHARCOT (EPPLEY)									
Average (SD)	0.299	(0.109)					15.00	35.00	14
Geometric Mean (GSD)	0.273	(1.635)							
CHARTERER (No. 289)									
Average (SD)	0.245	(0.126)	0.214	(0.120)	0.273	(0.162)	14.48	30.55	43
Geometric Mean (GSD)	0.216	(1.661)	0.186	(1.718)					
ENDURER (No. 280)									
Average (SD)	0.263	(0.169)	0.213	(0.168)	0.545	(0.362)	15.33	23.27	39
Geometric Mean (GSD)	0.223	(1.769)	0.166	(2.043)					
GILLISS (No. 282)									
Average (SD)	0.139	(0.119)	0.121	(0.122)	0.492	(0.613)	9.31	24.62	30
Geometric Mean (GSD)	0.111	(1.887)	0.086	(2.272)					
MATAMORAS (No. 271)									
Average (SD)	0.098	(0.057)	0.055	(0.042)	1.168	(0.557)	6.80	47.58	31
Geometric Mean (GSD)	0.085	(1.706)	0.044	(1.907)					
OCEANOGRAPHER (EPPLEY No. 56)									
Average (SD)	0.069	(0.034)					9.21	23.57	11
Geometric Mean (GSD)	0.057	(2.225)							
RESEARCHER (EPPLEY No. 52)									
Average (SD)	0.077	(0.037)					7.47	23.69	41
Geometric Mean (GSD)	0.066	(1.973)							
SALDANHA (No. 275)									
Average (SD)	0.106	(0.036)	0.067	(0.022)	0.821	(0.356)	1.40	36.24	52
Geometric Mean (GSD)	0.100	(1.421)	0.064	(1.418)					
SIRIUS (No. 274)									
Average (SD)	0.196	(0.072)	0.144	(0.072)	0.759	(0.437)	7.86	38.81	56
Geometric Mean (GSD)	0.184	(1.441)	0.127	(1.690)					

thickness; extrapolation of the meter reading to zero air mass yields $I_{0\lambda}$. However, conditions of relatively constant low turbidity of sustained duration are only obtainable at a limited number of locations. Thus, most instruments, including ours, are calibrated against a limited number of these reference instruments which have been properly calibrated by the Langley method.

An extensive series of intercalibrations were made between our Volz instruments and two EPA reference instruments belonging to E. Flowers (NOAA); the EPA instruments are periodically calibrated by the Langley method at suitable locations in the western United States. Unfortunately the EPA and Volz instruments had only the 500 nm channel in common. In order to check the calibration of the 880 nm channel, we followed the Langley procedure.

Instruments were recalibrated in the Fall after the completion of GATE. Stability was found to be good for most instruments. Of the 13 Volz instruments tested and used in GATE, in the green channel, five drifted less than 2% and five drifted between 2 and 5%. In the red channel, six drifted less than 2% and three between 2 and 5%.

Also included in this work is data from two other types of instruments. On the Charcot, a two-channel (380 nm, 500 nm) Eppley sun photometer was used which was the same type employed in the United States EPA network. Also, five specially constructed (GATE) Eppley sun photometers were employed on four ships (Gilliss, Dallas, Researcher, and Oceanographer) and on Sal Island as a part of Carlson's radiation study there. The GATE Eppleys had two bands (380 and 500 nm), were solar tracking and the output was continuously recorded.

8.5 AEROSOL MEASUREMENTS

A detailed discussion of the aerosol sampling and analysis procedure is presented in Savoie and Prospero (1977). In summary, daily 24-hour duration bulk aerosol samples were collected on 6 cm effective diameter IPC-1478 filters at flow rates of 1.1–1.3 standard cubic metres per minute. In order to reduce the filter blank, the filters were subjected to a series of extractions to remove acid- and water-soluble species prior to being used.

In the analysis procedure, a quarter section of each filter was taken and the water-soluble material removed in a series of three extractions. The extractions and filtration of the resulting solutions were performed in a centrifugal filtration device fitted with a 25 mm membrane filter.

The mineral aerosol component was measured by ashing (500°C) the extracted IPC filter and the membrane filter used to filter the extraction aliquots.

8.6 RESULTS AND DISCUSSION

The mean atmospheric turbidity parameters for all stations are presented in Table 8.1. The data for the land stations is broken down into phases in Table 8.2. The dates of the phases were: I – 26 June to 18 July; II – 19 July to 19 August;

TABLE 8.2 Atmospheric Turbidity Parameters for the North Atlantic during Each Phase of GATE (Land Stations: Summer, 1974)

Site (Photometer No.) Parameters	Phase I							Phase II							Phase III						
	B(500)		*B*(880)		Alpha		*n*	*B*(500)		*B*(880)		Alpha		*n*	*B*(500)		*B*(880)		Alpha		*n*
BARBADOS (No. 281)																					
Average (SD)	0.173	(0.090)	0.154	(0.086)	0.254	(0.178)	16	0.144	(0.087)	0.127	(0.079)	0.262	(0.215)	32	0.093	(0.057)	0.080	(0.056)	0.364	(0.282)	31
Geometric Mean (GSD)	0.149	(1.882)	0.129	(1.948)				0.118	(1.959)	0.102	(2.044)				0.079	(1.807)	0.064	(1.974)			
BERMUDA (No. 32)																					
Average (SD)	0.116	(0.012)	0.065	(0.018)	1.067	(0.465)	4	0.088	(0.080)	0.039	(0.033)	1.488	(0.454)	24	0.098	(0.020)	0.038	(0.016)	1.748	(0.415)	25
Geometric Mean (GSD)	0.115	(1.111)	0.063	(1.330)				0.076	(1.535)	0.033	(1.621)				0.096	(1.217)	0.036	(1.464)			
DAKAR (No. 278)																					
Average (SD)	0.350	(0.125)	0.328	(0.133)	0.152	(0.210)	12														
Geometric Mean (GSD)	0.330	(1.434)	0.303	(1.547)																	
MIAMI (No. 101)																					
Average (SD)	0.122	(0.052)	0.081	(0.032)	0.735	(0.412)	17	0.106	(0.055)	0.070	(0.051)	0.871	(0.298)	26	0.074	(0.037)	0.044	(0.024)	0.946	(0.472)	29
Geometric Mean (GSD)	0.112	(1.511)	0.075	(1.525)				0.097	(1.499)	0.059	(1.716)				0.069	(1.431)	0.040	(1.511)			
SAL (No. 273)																					
Average (SD)	0.364	(0.136)	0.316	(0.134)	0.295	(0.200)	13	0.300	(0.075)	0.253	(0.076)	0.302	(0.073)	2	0.262	(0.087)	0.208	(0.077)	0.429	(0.154)	18
Geometric Mean (GSD)	0.341	(1.479)	0.288	(1.600)				0.296	(1.286)	0.248	(1.355)				0.242	(1.590)	0.189	(1.673)			
SAL (No. 276)																					
Average (SD)	0.331	(0.151)	0.295	(0.144)	0.220	(0.071)	2	0.266	(0.113)	0.224	(0.102)	0.343	(0.158)	25	0.257	(0.087)	0.210	(0.076)	0.382	(0.136	18
Geometric Mean (GSD)	0.314	(1.603)	0.277	(1.667)				0.245	(1.546)	0.202	(1.628)				0.237	(1.607)	0.190	(1.709)			
SAL (EPPLEY)																					
Average (SD)	0.336	(0.102)					10	0.241	(0.100)					20							
Geometric Mean (GSD)	0.323	(1.345)						0.223	(1.521)												

Phase I: 26 June – 18 July; Phase II: 19 July – 19 Aug.; Phase III: 20 Aug. – 23 Sept.

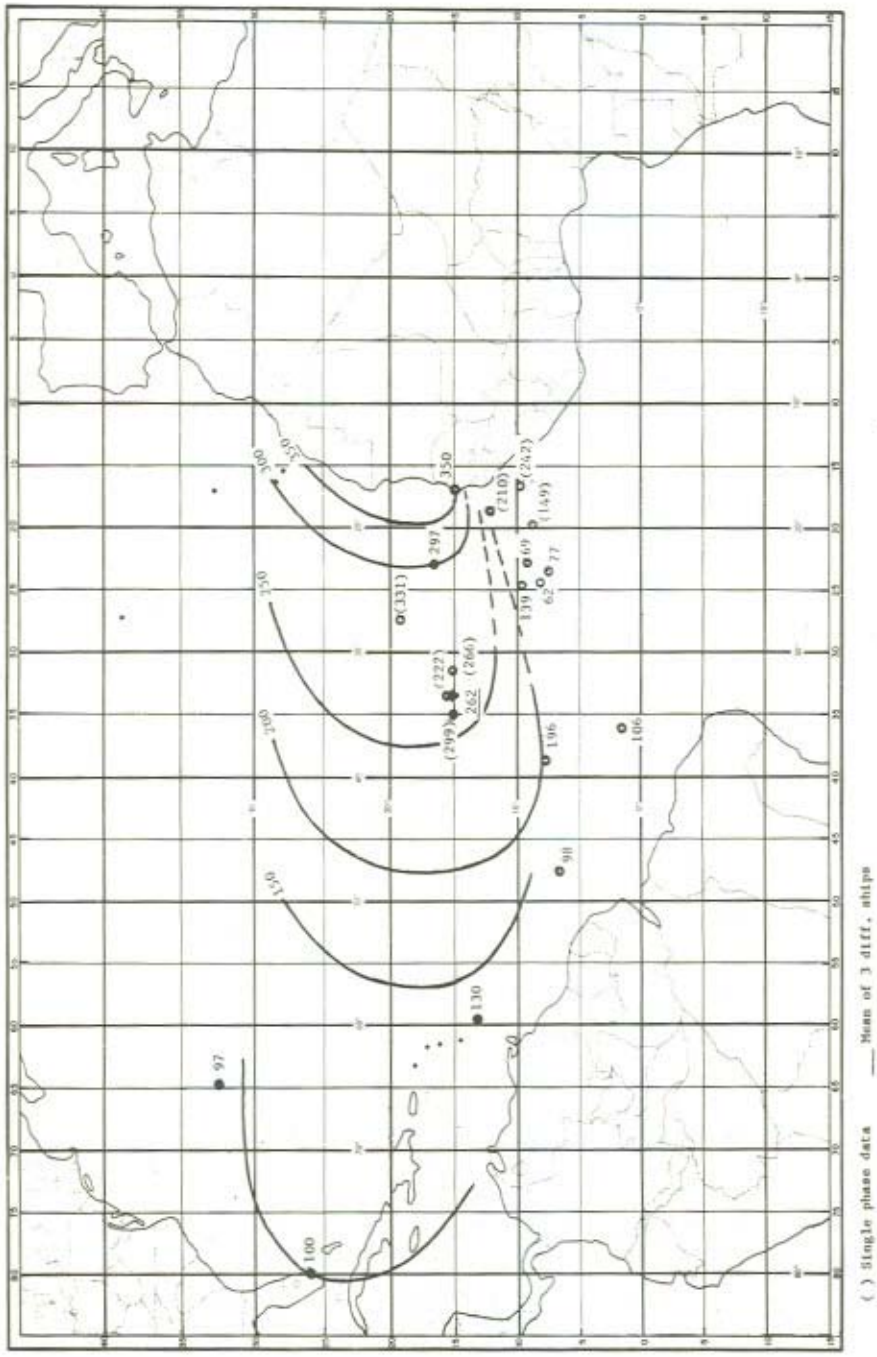

Figure 8.1 Volz turbidity, arithmetic mean values ($\times 10^3$) for GATE

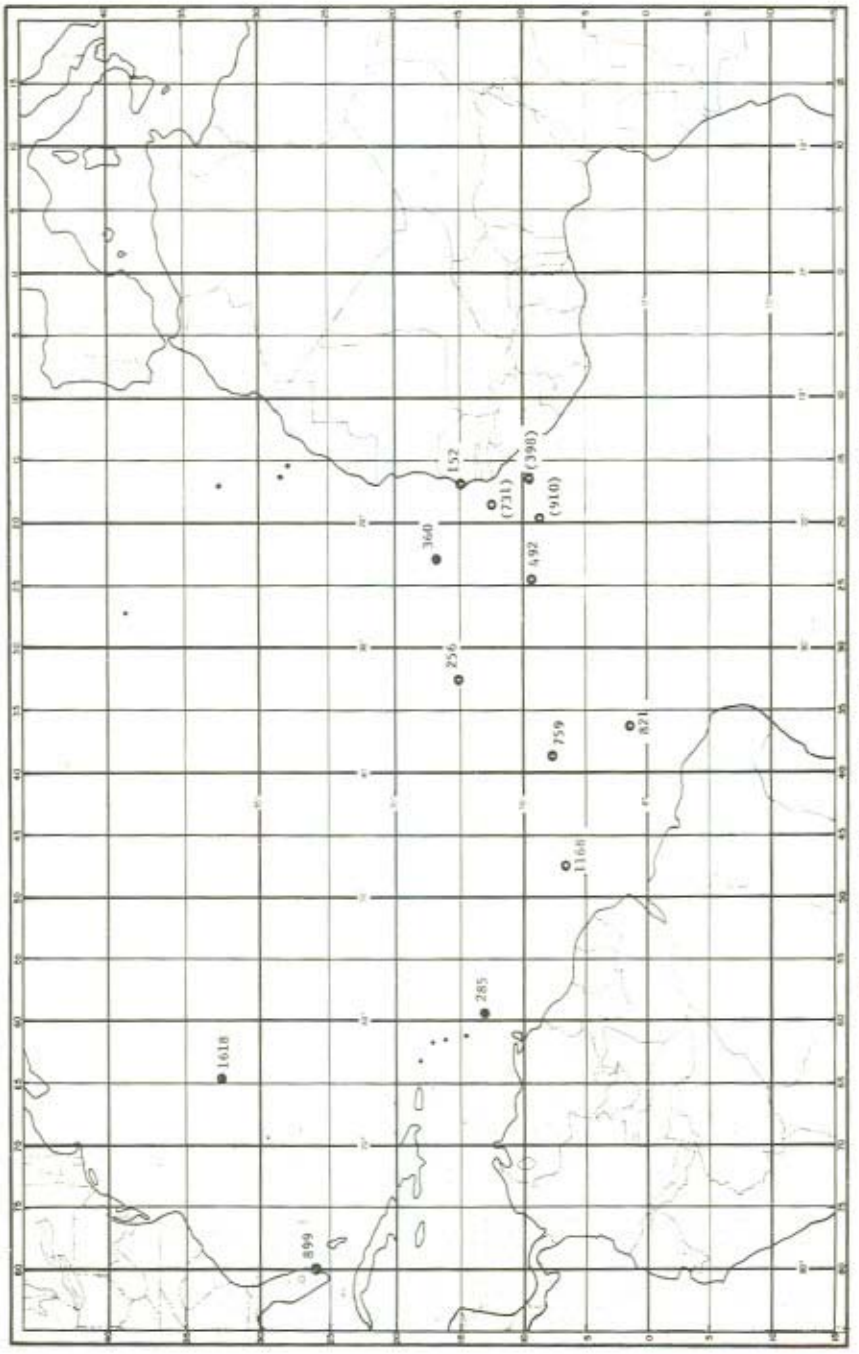

Figure 8.2 Alpha, arithmetic mean values ($\times 10^3$) for GATE

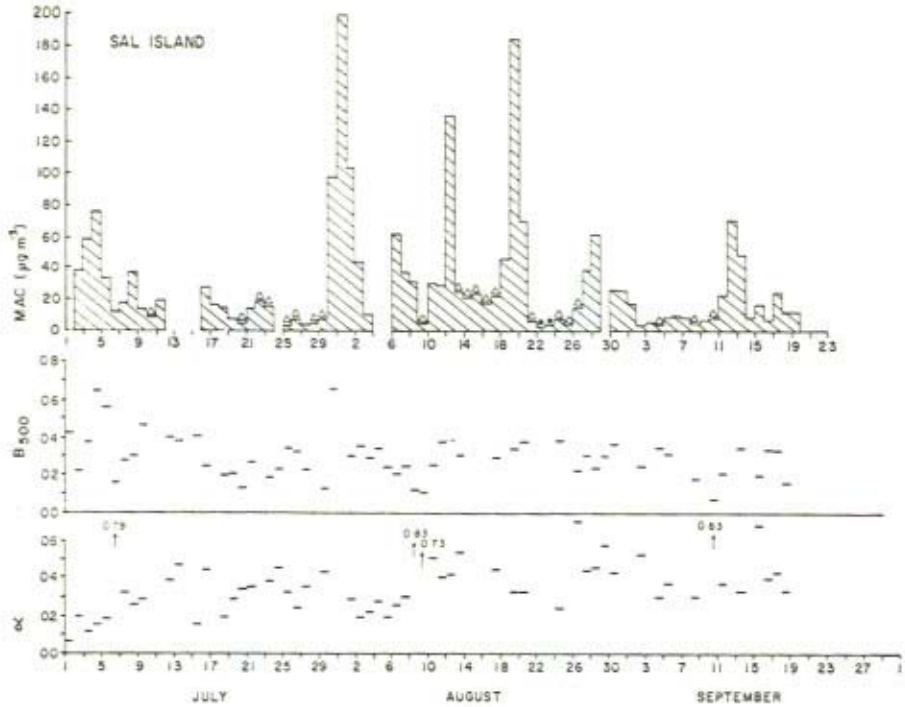
SAL ISLAND
MAC (μg m⁻³)
B500
α
JULY
AUGUST
SEPTEMBER

(a)

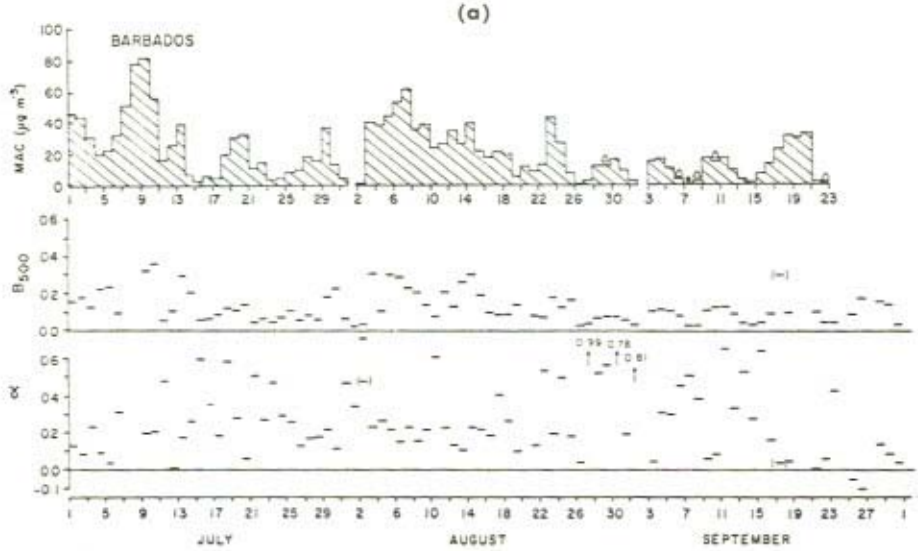
BARBADOS
MAC (μg m⁻³)
B500
α
JULY
AUGUST
SEPTEMBER

(b)

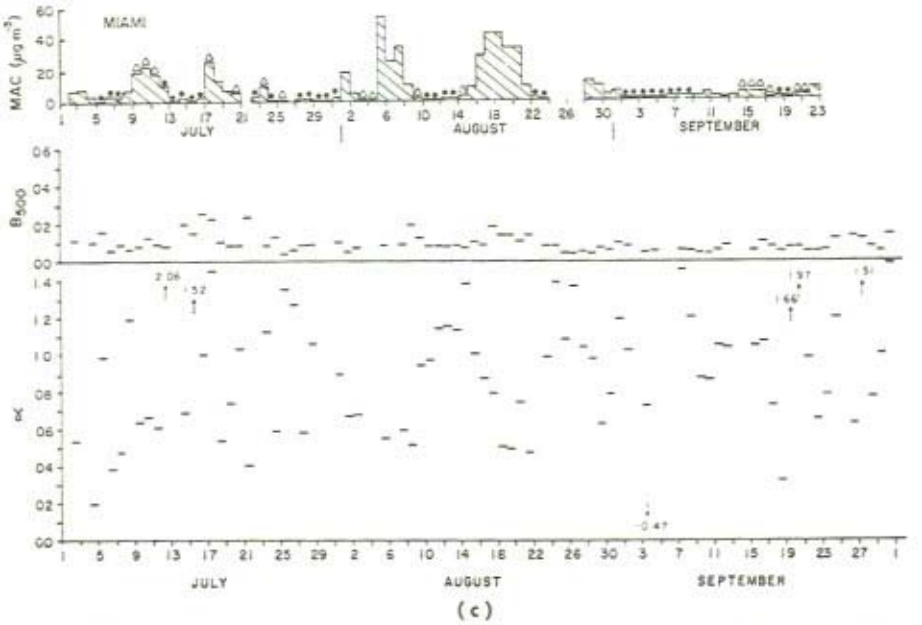

Figure 8.3 Daily values of mineral aerosol concentration (10^{-6} g m^{-3}), Volz turbidity at 500 nm and alpha

III – 20 August to 23 September. The mean values of the turbidity at 500 nm and of alpha are presented in Figures 8.1 and 8.2, respectively. As seen in Figure 8.1, the turbidity is greatest along the west coast of Africa and decreases with distance westward across the Atlantic and southward to the intertropical convergence zone (ITCZ). The high turbidities are attributable to the presence of large concentrations of mineral aerosol in the atmosphere. The daily values of mineral aerosol, turbidity (500 nm) and alpha at Sal, Barbardos, and Miami are shown in Figures 8.3a, b, c. The mineral aerosol data are coded according to filter colour, all filters being red-brown except those marked (●) indicating black or (△) indicating a mixed colour of red-brown and black. The vast majority of the Sal and Barbados aerosol samples are red-brown, a colour that is characteristic of Saharan aerosols. In contrast, Miami aerosols are predominantly characterized by a black or mixed colour. Nonetheless, on a mass basis, the dominant mineral aerosol component in Miami is Saharan dust.

The large day-to-day variations in dust load at Sal, Barbardos, and Miami are attributable to the passage of dust-laden air parcels associated with Saharan air outbreaks (SAO). The movement of these outbreaks can be observed by means of SMS-1 satellite photographs. The turbidity isopleths in Figure 8.1 are partially based on such photographs.

The turbidity values at Sal, Barbados, and Miami are not highly correlated with

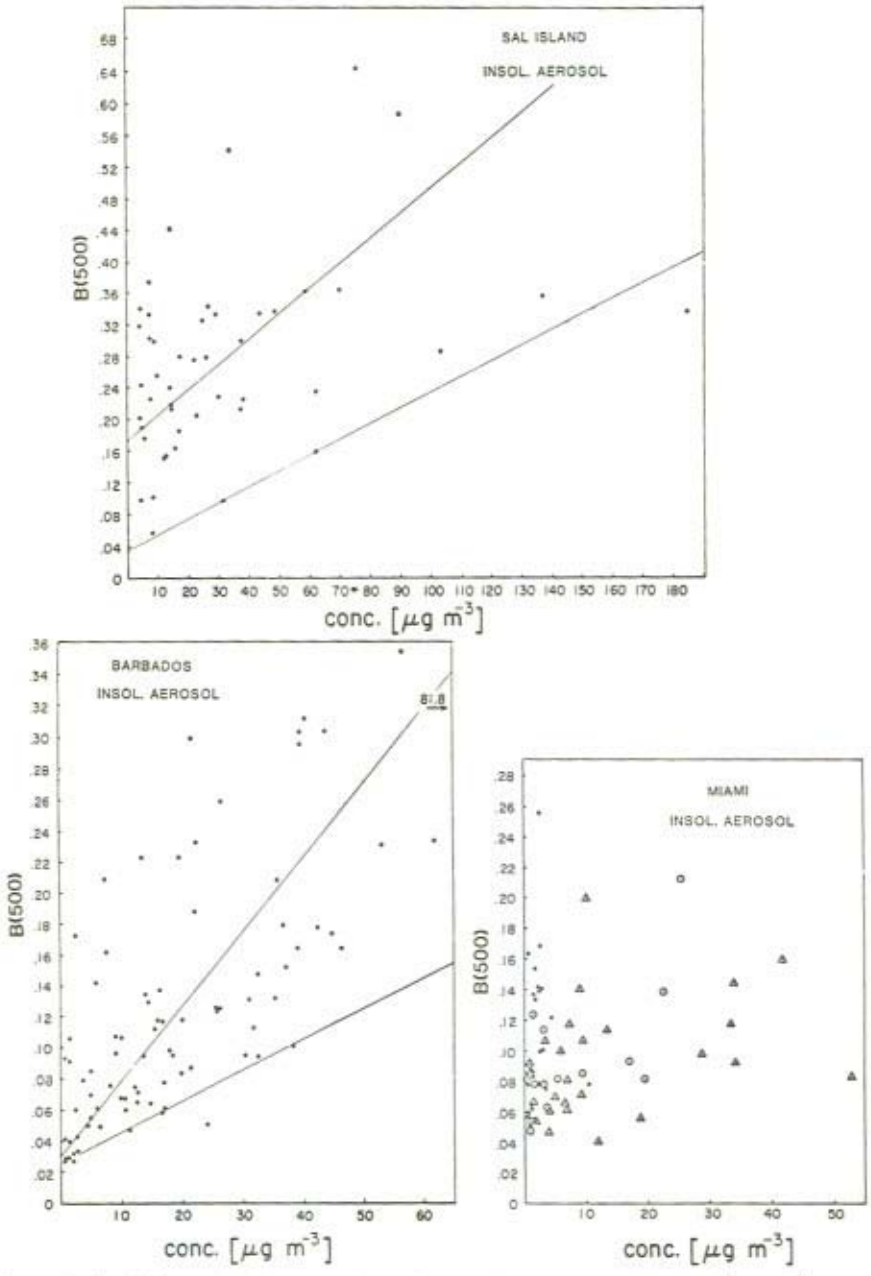

Figure 8.4 Volz turbidity *vs.* mineral aerosol concentration (10^{-6} g m^{-3}). The upper line in the Figures Sal Island and Barbados represents a least squares fit to the data points. The lower line is drawn by eye to show the trend of the lower limit of B *vs* aerosol concentration

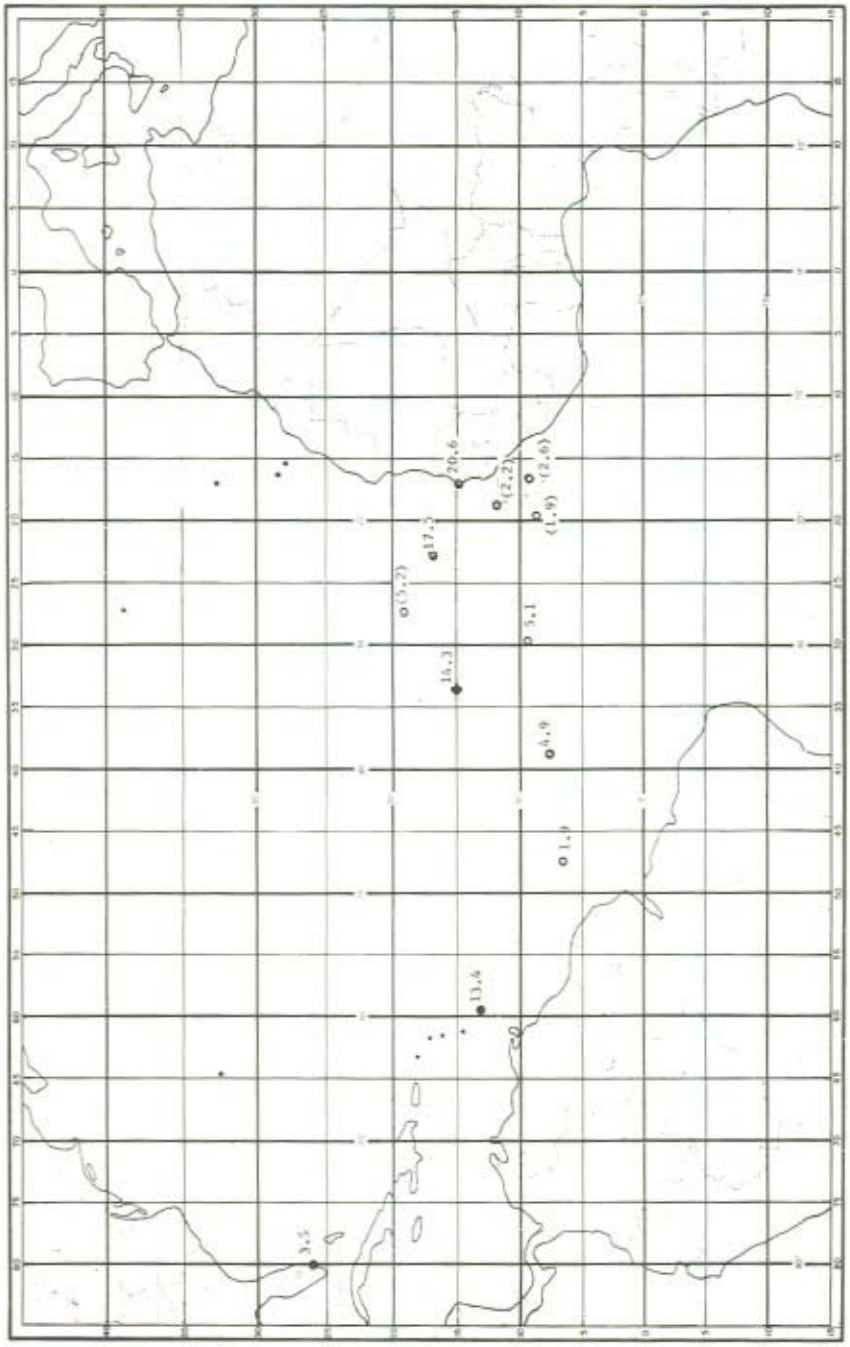

Figure 8.5 Mineral aerosol concentration (10^{-6} g m^{-3}), geometric mean values for GATE

the aerosol concentration as measured in surface level air. This can be noted from Figure 8.3; however, the lack of close correlation is best seen in Figures 8.4a, b, and c which show Volz turbidity *vs.* mineral aerosol concentration. (In Figure 8.4 the same symbols are used as in Figure 8.6.) Indeed, the mean mineral aerosol concentrations in the trade wind mixed layer at stations in the equatorial North Atlantic are not greatly different (see Table 8.3 and Figure 8.5). Concentrations drop sharply in the ITCZ and in the far western Atlantic (based on the Miami data).

The mineral aerosol and turbidity data is best understood in terms of the schematic model of Saharan dust transport proposed by Carlson and Prospero (1972). They suggest that the dust transport takes place primarily in a layer, the Saharan air layer (SAL), which has a base at 1 to 1.5 km and a top at 5 to 7 km. Dust is transported downward by gravitation (most effective for particles above *ca.* 10 μm) and by downward mixing through convective erosion of the SAL base.

The two-layer model explains a number of otherwise curious features in the data. Compare, for example, the phase I mineral aerosol data (Table 8.3) for the Endurer, which was located at 19°05′N 27°20′W, with that on Sal Island or on the Charcot at 15°00′N 35°00′W. Although the Endurer dust concentration is only a third to a quarter of those at the other two stations, the arithmetic mean turbidities are quite comparable: 0.331, 0.364 and 0.299 respectively. Thus, the SAL overlies all three stations and the vertically integrated aerosol loading in the optically active size range is relatively constant. However, the low level winds, which have a relatively strong northerly component in this region, have accumulated relatively little dust 'fallout' in the relatively short traverse under the layer.

TABLE 8.3 Mineral Aerosol Concentrations for the Equatorial North Atlantic During GATE

	Phase I			Phase II			Phase III			Overall		
Station	*AM*	*GM*	*n*	*AM*	*GM*	*n*	*AM*	*GM*	*n*	*AM*	*GM*	
Land:												
Barbados	31.8	23.1	21	24.7	18.9	31	12.0	7.0	34	21.4	13.4	8
Dakar				38.3	31.1	11	17.2	9.7	6	30.9	20.6	1
Miami	9.2	5.9	16	11.6	4.6	26	4.1	2.0	27	8.1	3.5	6
Sal	28.9	23.8	13	41.7	22.1	29	18.3	12.0	29	29.8	17.5	7
Ship:												
Charcot	20.2	15.1	22							20.2	15.1	2
Charterer	5.3	2.6	14	41.8	28.3	23	15.1	7.8	28	22.4	9.7	6
Endurer	17.9	5.2	22	5.1	2.2	21	2.2	1.9	6	10.5	3.2	4
Gilliss	24.5	19.4	22	8.4	2.2	13	5.4	2.4	25	13.1	5.1	6
Matamoros				1.7	0.78	23	11.8	4.6	24	6.9	1.9	4
Sirius	19.8	16.0	21	3.7	1.4	21	9.9	5.3	19	11.2	4.9	6

Phase I: 26 June–18 July; Phase II: 19 July–19 Aug.: Phase III: 20 Aug.–23 Sept.

AM = Arithmetic mean; GM = Geometric mean.

The values of the Angstrom wavelength exponent, α (Tables 8.1 and 8.2, Figure 8.2) are relatively constant in the trade wind belt. Error analysis suggests that there is no significant difference amongst the mean values at Sal (0.360), at the composite ship position at 15°N 32°30′W (0.256) and at Barbardos (0.285). These low alphas, and the attendant neutral extinction, suggest that the Junge size distribution parameter, β, is close to two. This is in agreement with size distribution measurements made by Savoie and Prospero (1976) who found that the normalized geometric mean particle number-size distributions for three major dust outbreaks passing over Sal had $\beta = 2.02 \pm 0.29$ in the size range 0.5 to 1.0 μm diameter. In contrast, non-arid region aerosols have β values in the range 3 to 3.5 which should yield α values of 1 to 1.5. Alpha values in the latter range are seen in Miami during those periods when Saharan aerosols are not present in significant concentration; conversely, there is a tendency for low α's to obtain when Saharan air parcels are in the area. The relationship of α to Saharan aerosol concentration is best seen in Figure 8.6; here, the data points are coded according to colour with the symbol (△)

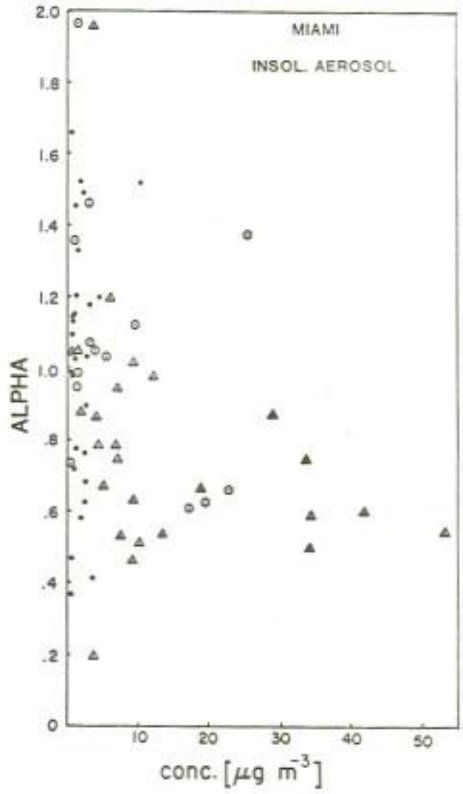

Figure 8.6 Alpha *vs.* mineral aerosol concentration (10^{-6} g m^{-3}), Miami

representing red-brown aerosol, (○) representing black and (●) representing mixed black and red-brown. There is a clear tendency for low α's to occur in association with red-brown aerosol and high α's in association with black aerosol. There is a certain degree of ambiguity in the relationship because of the fact that the surface level air may not be very representative of the vertically integrated aerosol at the site. Nonetheless, of the 28 days when α was greater than 1, black aerosols dominated on 15 days, mixed colour on eight and red-brown on five. Of the 39 days when α was less than one, black occurred on 12, mixed on six and red-brown on 21.

The persistence of low α's in Barbados and Miami in the presence of Saharan air parcels is consistent with the size distribution measurements at these locations; although the mean β's for the size range 0.5–1 μm were somewhat higher than that at Sal, the differences were not significant and the combined mean for all three stations was 2.18 ± 0.13 (Savoie and Prospero, 1976). Low α values appear to be a characteristic feature of air masses over, or emanating from, arid regions (Roosen *et al.*, 1973).

8.7 ACKNOWLEDGEMENT

Research supported by the Global Atmospheric Research Program, National Science Foundation (grant ATM76-01195) and the GATE Project Office, NOAA.

REFERENCES

Carlson, T. N., and Prospero, J. M. (1972). The large-scale movement of Saharan air outbreaks over the northern equatorial Atlantic. *J. Appl. Meteorol.*, **11**, 283–297.

Roosen, R. B., Angione, R. J., and Klemck, C. H. (1973). Worldwide variations in atmospheric transmission: I. Baseline results from Smithsonian observations. *Bull. Am. Meteorol. Soc.*, **54**, 307–316.

Savoie, D. L., and Prospero, J. M. (1976). Saharan aerosol transport across the Atlantic Ocean: characteristics of the input and the output. *Bull. Am. Meteorol. Soc.*, **57**, p. 145.

Savoie, D. L., and Prospero, J. M. (1977). Aerosol concentration statistics for the northern equatorial Atlantic, *J. Geophys. Res.*, in press.